

EFFECT OF ENVIRONMENT ON FRACTURE - MECHANISMS OF LIQUID-METAL
EMBRITTELEMENT, STRESS-CORROSION CRACKING AND CORROSION-FATIGUE

S. P. Lynch*

INTRODUCTION

Many environments induce sub-critical crack growth resulting in fractures associated with less ductility, and often different fracture paths and modes, than fractures in inert environments. Proposed explanations for these effects are discussed in reviews of liquid-metal embrittlement (LME) [1], stress-corrosion cracking (SCC) [2] and corrosion-fatigue [3]. In the present paper, a new explanation for LME is proposed on the basis of metallographic and fractographic studies. Evidence suggests that this proposed mechanism could also be relevant to SCC, hydrogen embrittlement (HE) and corrosion-fatigue.

EXPERIMENTAL PROCEDURE

High-purity aluminium single crystals and Al-Zn-Mg (6.27 wt.-%Zn, 294 wt.-%Mg) polycrystals were studied. Aluminium specimens (Figure 1) were notched, using a fine saw, in the presence of liquid metal and then immediately tested in cantilever bending. (There was insufficient time for significant diffusion of liquid-metal atoms into the crystals). Crack growth in Al-Zn-Mg polycrystals was studied using bolt-loaded, double-cantilever-beam (DCB) specimens (Figure 2); specimens were solution-treated at 430°C, quenched in boiling water, aged at 100°C for (A) 2 min. and (B) 60 min., then aged at 180°C (in oil) for 120 min. These heat treatments (H.T.) produce (i) fine dispersions of η -phase precipitates in grain interiors, (ii) η -phase precipitates at grain boundaries and (iii) precipitate-free zones (PFZs), (A) ~0.2 μ m and (B) ~0.05 μ m wide, adjacent to grain boundaries.

Environments used were (i) a liquid alloy** (44.7 wt.-%Bi, 22.6%Pb 19.1%In, 8.3%Sn, 5.3%Cd) (Melting point ~ 47°C), (ii) saturated aqueous potassium-iodide solution, and (iii) water-vapour/air at 20% relative humidity (R.H.). Tests were performed at ~ 50°C in the liquid alloy and at ~ 20°C in the other environments. Liquid alloy was removed from fractures by a jet of hot water; fracture surfaces were cleaned further by immersion in concentrated nitric acid for 1 min. and by stripping plastic replicas from the surfaces.

**Liquid mercury and liquid gallium produced similar results; using the liquid alloy facilitated experimentation.

*Aeronautical Research Laboratories, Department of Defence, Box 4331, G.P.O., Melbourne 3001, Australia.

EXPERIMENTAL OBSERVATIONS

Aluminium single crystals

Complete fracture of specimens occurred after bending $\sim 20-30^\circ$ in liquid alloy, while bending (up to 90°) in air produced blunting at the notch root without appreciable crack growth. After LME, fractures (Figure 3) were macroscopically flat and parallel to $\{100\}$ surfaces except for steps (river marks), in agreement with results of Westwood et al. [4]. On a microscopic scale, the fracture surfaces were completely covered by shallow, slightly elongated dimples; slip traces were also evident (Figure 4). Experiments showed that wetting surfaces with liquid alloy and removing the alloy had no significant effects on surface topography (Figure 4, inset).

Polishing the sides of specimens partially cracked in liquid alloy and then increasing the crack-opening displacement (COD), to produce an increment of crack growth in liquid alloy, showed that considerable slip occurred during fracture surfaces appeared the same at the edges of specimens as at the centre, slip at the surface is probably reasonably indicative of the deformation occurring during crack growth in the centre of specimens. (Some slip at the surface, however, is associated with through-the-thickness flow). After liquid alloy had been removed from the crack, the specimen was repolished and then the COD increased in air (at 20°C , traces of alloy remaining will be solid). This procedure resulted mainly in blunting of the crack tip, without much crack growth (Figure 6).

Al-Zn-Mg Polycrystals

Very rapid ($\sim 10\text{mm/sec}$) sub-critical (inter crystalline) crack growth was induced when DCB specimens, pre-cracked in air and loaded to near K_{IC} , were 'wet' with liquid alloy (Figure 2). Dimpled fracture surfaces, and appreciable deformation in grains adjacent to cracks, were observed after LME (H.T. 'A'); dimples were generally smaller, shallower, and more elongated than dimples on fractures due to overload (Figure 7).

DISCUSSION

Mechanism of LME

LME has previously been considered [1,4] as a special case of a general criterion [5] that the σ/τ ratio governs ductile versus brittle behaviour. It has been assumed that chemisorption of liquid-metal atoms lowers the tensile strength, σ , of atomic bonds at crack tips (but does not affect the shear stress, τ , required to move dislocations) so that crack growth occurs by repeated adsorption and breaking of bonds at low applied stress. Fracture surfaces produced by such a 'bond-rupture' process would be flat and little deformation would be associated with fracture. It is implicit that dislocations moving in the stress fields of such cracks do not generally intersect crack tips or cause blunting.

The present studies of LME show slip densities and distributions which suggest that dislocations do intersect crack tips. Moreover, dimpled fracture surfaces indicate that microvoids nucleate and grow ahead of cracks and, hence, that some blunting does occur at crack tips. Observations of LME in aluminium single crystals suggest that crack growth occurs by alternate shear on $\{111\}$ slip planes intersecting crack tips with sufficient general strain accompanying crack growth to produce some blunting and growth of microvoids. (Other workers [6-8] have also proposed that,

under certain conditions, cracks can grow by alternate shear with the production of cleavage-like $\{100\}$ fracture surfaces). Observations on Al-Zn-Mg polycrystals following critical (overload) and sub-critical crack growth (LME) indicate that fracture involves the concentration of deformation in PFZs causing microvoid coalescence (MVC). Crack growth, in liquid-metal environments, by MVC was also observed in other materials [9]. Thus, it is concluded that fracture in embrittling liquid-metal environments generally occurs by plastic flow (shear movement of atoms) rather than by tensile separation of atoms at crack tips.

LME could be explained on the basis that chemisorption of liquid-metal atoms facilitates nucleation and movement of dislocations on slip planes intersecting crack tips. There is evidence [10] that, since atoms at surfaces (in vacuum) have fewer neighbours than atoms in the interior, the lattice-spacings in the first few atomic layers differ from those in the interior. It has been suggested [11] that such 'surface-lattice distortion' should hinder the nucleation and egress of dislocations at surfaces. Since chemisorption of environmental species at surfaces should reduce this 'surface-lattice distortion' [12], nucleation and egress of dislocations at surfaces (crack tips) should be facilitated by adsorption.

Adsorption-activated dislocation nucleation/movement on slip planes intersecting crack tips would produce sub-critical crack growth (by shear) and also result in fractures with reduced ductility (less crack-tip blunting)*. Extensive blunting at tips of cracks, in specimens below general yield, requires a general strain in the plastic zone ahead of cracks, and hence, generally necessitates slip on at least five independent systems which freely interpenetrate and cross-slip [13]; crack growth by alternate shear requires slip on only two slip planes intersecting crack tips. The balance between crack growth and crack-tip blunting (both relax elastic strain energy around cracks) should therefore be determined by the relative proportions of slip on planes intersecting crack tips compared to 'general' slip ahead of cracks; larger proportions of the former, which is promoted by chemisorption, favour crack growth**.

The hydrogen (gas)-iron (solid) couple satisfies most criteria suggested as pre-requisites for LME [14]. The mechanism proposed for LME in the present paper could therefore be applicable to HE (although HE is more complex than LME since hydrogen can readily diffuse into materials). This proposal is consistent with many characteristics of HE and, in particular, with observations [15] of iron surfaces in the presence of hydrogen using field-ion microscopy; this work suggests that nucleation of dislocations is catalysed by adsorption of hydrogen.

Stress-corrosion cracking and corrosion-fatigue

Analogies between SCC and LME suggest that similar mechanisms are involved in both effects [16], e.g., cleavage-like fractures are observed for aluminium single crystals in liquid metals, austenitic steels in boiling MgCl_2 , titanium alloys in methanol, and others. Thus, a mechanism of adsorption-induced alternate shear, producing cleavage-like fracture surfaces, could be applicable to many cases of SCC. Previous objections [2] to an 'adsorption-induced cleavage' mechanism of SCC were based on the unlikely operation of a 'bond-rupture' process during SCC.

*An effect of adsorption on flow behaviour of uncracked specimens, with small surface-to-volume ratios, would not be expected and is not observed.
**A criterion for ductile versus brittle behaviour based on distributions of slip around cracks may be generally applicable.

The case for a common mechanism for LME and SCC, in Al-Zn-Mg, is supported by the following observations. Immersion of pre-cracked and loaded (to near K_{IC}) DCB specimens (H.T. 'B') in KI solution resulted in an increment ($\sim 1\text{mm}$) of very rapid ($\sim 10\text{mm/sec}$) intercrystalline crack growth within 1 sec. of immersion. This burst of rapid crack growth is *sub-critical* cracking induced by the environment since (i) stress intensity decreases with increasing crack length in the specimens used, (ii) similarly loaded specimens in water-vapour/air environments show only slow crack growth and, hence the rapid growth in aqueous solutions is unlikely to be due to overload fracture initiated by the environment (e.g. by sharpening the crack tip), and (iii) the *initial* burst of rapid cracking cannot be overload fracture of a ligament lagging behind the main crack front. The very rapid initial rates of sub-critical crack growth in KI solution (as in LME) strongly suggest that adsorption is responsible; other proposed mechanisms of SCC involving dissolution, diffusion of hydrogen ahead of cracks, oxide film formation/fracture, are unlikely to have time to occur.

SCC of Al-Zn-Mg (H.T. 'A') in water-vapour/air (20% R.H.) produces entirely dimpled fracture surfaces (Figure 8); dislocation nucleation/movement at crack tips, activated by adsorbed water molecules, would explain this observation. Dissolution cannot be involved since there is no liquid electrolyte at crack tips at 20% R.H. and there is no really convincing evidence that diffusion of hydrogen ahead of cracks is involved in SCC of aluminium alloys [9].

In some instances, other mechanisms of SCC could occur in conjunction with, and contribute to, crack growth by adsorption-induced slip.

There is evidence that corrosion-fatigue involves an effect of adsorption at crack tips [17]. Here, 'brittle' striations, often on {100} fracture surfaces and associated with increased rates of crack growth, are observed after fatigue in both liquid-metal [9,18] and aqueous environments; 'ductile' striations are usually produced by fatigue in air. Adsorption-activated dislocation nucleation/movement would explain these results and could provide a generally consistent explanation for the effects of environment on fracture.

REFERENCES

1. KAMDAR, M.H., Progress in Materials Science, 15, 1973, 289.
2. SCULLY, J.C. (ed.), The Theory of Stress Corrosion Cracking in Alloys, Publ. NATO, Brussels, 1971.
3. DEVEREUX, O.F., McEVILY, A.J. and STAEHLE, R.W., (eds.), Corrosion Fatigue: Chemistry, Mechanisms and Microstructure Publ. NACE, 1971.
4. WESTWOOD, A.R.C., PREECE, C.M. and KAMDAR, M.H., Trans. ASM, 60, 1967, 723.
5. KELLY, A., TYSON, W.R. and COTTRELL, A.H., Phil. Mag., 15, 1967, 567.
6. PELLOUX, R.M.N., Eng. Frac. Mechanics, 1, 1970, 697.
7. NEUMANN, P., Acta Met., 22, 1974, 1155.
8. GARRETT, G.G. and KNOTT, J.F., Acta Met., 23, 1975, 841.
9. LYNCH, S.P., ARL Report, to be published
10. LATANISION, R.M., p. 185, ref. 3.
11. FLEISCHER, R.L., Acta Met., 8, 1960, 598.
12. UHLIG, H.H., Metal Interfaces, Publ. ASM, 1952, 312.
13. CONGLETON, J., PETCH, N.J. and SHIELS, S.A., Phil. Mag., 19, 1969, 795.

14. WILLIAMS, D.P. and NELSON, H.G., Met. Trans., 1, 1970, 63.
15. CLUM, J.A., Scripta Met., 9, 1975, 51.
16. NICHOLS, H. and ROSTOKER, W., Trans. ASM, 56, 1963, 494.
17. PELLOUX, R.M.N., Fracture, Brighton (Chapman and Hall), 1969, 731.
18. WANHILL, R.J.H., Corrosion, 31, 1975, 66.

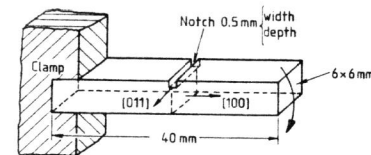


Figure 1 Aluminium single crystal specimens showing approximate orientation and direction of applied bending load.

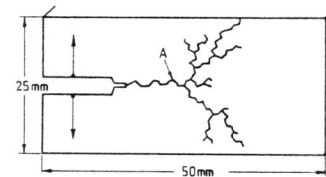


Figure 2 Al-Zn-Mg DCB specimen, pre-cracked in air to 'A', illustrating type of cracking configuration produced by LME.

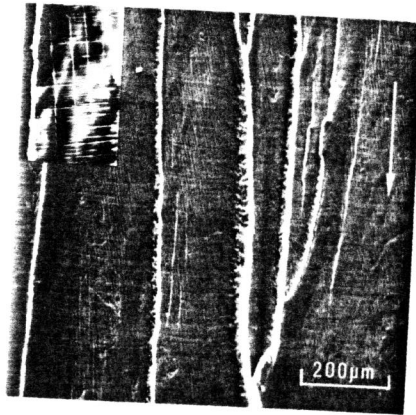


Figure 3 Fractograph (SEM) of Al. single crystal cracked in liquid alloy. Insert (optical micrograph) shows fracture surface after electropolishing and straining slightly; orthogonal network of slip traces indicates that the surface is macroscopically parallel to {100}.

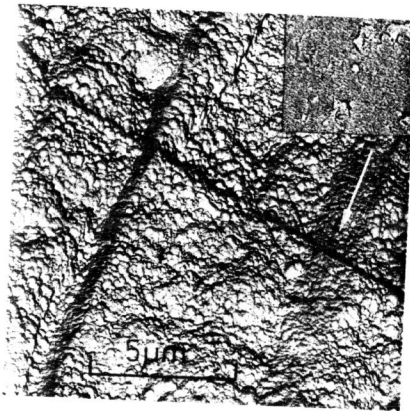


Figure 4 Fractograph (EM)* of Al. single crystal cracked in liquid alloy showing dimples and slip traces. Insert (EM) shows electropolished aluminium surface after 'fluxing' in NaOH, wetting with liquid alloy, and removing liquid alloy showing flat surface except for pitting produced by NaOH.

*EM - Electron micrographs of secondary-carbon replicas. Arrows show direction of crack growth.

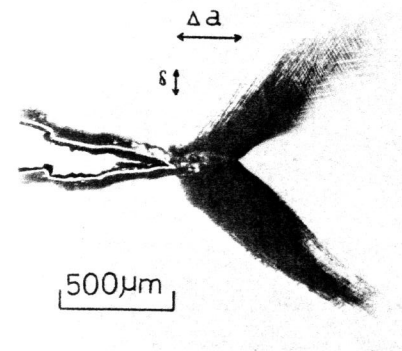


Figure 5 Optical micrograph showing slip associated with crack growth in Al. single crystal in liquid-alloy environment; except for the first 10-20μm, little slip occurs directly ahead of the crack. Crack profile before COD was increased has been superimposed (crack is filled with alloy).

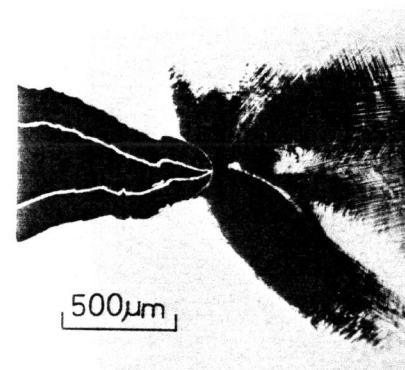


Figure 6 Optical micrograph of crack shown in Figure 5 after removing liquid alloy, repolishing, and increasing COD in air showing considerable slip ahead of crack associated with blunting. Crack profile before blunting has been superimposed.



Figure 7 Fractograph (EM)* after sub-critical crack growth of Al-Zn-Mg in liquid alloy. Top insert (optical micrograph) shows deformation associated with sub-critical crack growth revealed by ageing after fracture, sectioning, polishing and etching. Bottom insert shows fractograph (EM) of critical (overload) crack growth in air (same magnification as main figure).

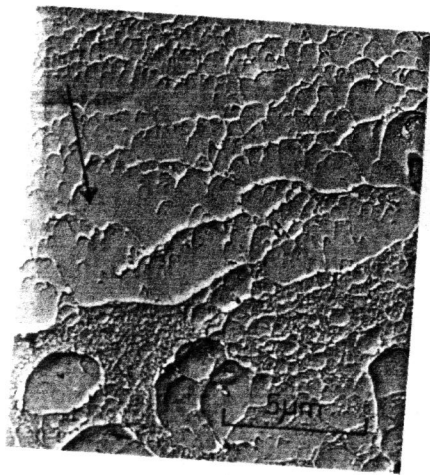


Figure 8 Fractograph (EM)* after sub-critical crack growth (at 'high' stress intensity) of Al-Zn-Mg in water-vapour/air (20% R.H.).

*EM - Electron micrographs of secondary-carbon replicas. Arrows show direction of crack growth.